University of HUDDERSFIELD
University of Huddersfield Press

Fields: journal of Huddersfield student research
Available open access at: https://www.fieldsjournal.org.uk/

FIELDS Journal of Huddersfield student research

High-resolution analysis of anti-migratory inhibitors in high-grade glioma treatment

Eryn Burns

University of Huddersfield, Queensgate, Huddersfield, HD1 3DH

ARTICLEINFO

Article history:
Received 25 March 2021
Received in revised form 18 October 2021
Accepted 07 April 2022

Keywords:
Cancer
Glioblastoma Multiforme
Glioma
Astrocytoma
Mesenchymal
Amoeboid

ABSTRACT

Glioblastoma Multiforme (GBM) is an extremely aggressive form of glioma tumour. The characteristically invasive properties of GBM contribute to the poor prognosis in sufferers. This study focuses on the therapeutic potential of four anti-migratory drugs: 6-bromo-indirubin-3'-oxime (BIO), CCG-1423, Latrunculin A (LAT A) and Lithium Chloride (LiCl), in vitro. The migration distances of GBM cells and cell circularity for each treatment and an untreated control were measured and statistically analysed. This was achieved using treated GBM spheroids of the U251 cell line and an untreated control. Spheroid sections were analysed in QuPath. This data was analysed in SPSS.

Each of the treatments showed significant statistical differences compared to the control spheroid for the migration distance measurements. LAT A was shown to have the greatest effect in decreasing the cell migration. Migrated cell circularity were significantly more rounded than the non-migrated cells for each treatment. The cell migration distance study suggests further study, to analyse the effects of these drugs in vivo. The 'cell circularity index' study should be amended to more accurately represent the changes in cell elongation due to morphological changes occurring as cells migrate from the tumour.

Introduction

According to the National Institute for Health and Care Excellence (NICE) approximately 30% of adults diagnosed with high-grade brain tumours (grades 3 and 4) survive for one year, and 13% survive for five years (NICE, 2005). These devastating statistics signify an urgent need to improve the prognosis of patients suffering from this disease. High-grade gliomas are tumours found within the brain tissue. They grow rapidly and characteristically can migrate from the original tumour site and invade other areas of the brain. This hallmark of cancer, as defined by Hanahan & Weinberg (2011), limits treatment options in this tumour type. Cells which have not been removed following initial surgery may migrate and spread, allowing tumours to recur (Liu et al., 2018). Recurrence of these tumours is the cause of death in patients. It follows that disease management must include the prevention of tumour dissemination and recurrence. Studies into the therapeutic modes of action of anti-migratory drugs are being developed to prevent the spread of the cells from the original tumour. Within this project, the established glioma cell line U251 was used for analysis of the effect of various anti-migratory inhibitors on cell migration in a 3D migration assay – carried out prior to this study for analysis. Cell-derived spheroids (small, lab-grown tumours) were used to identify potential candidates and characterise their effect on cell migration for novel combination therapies in the foreseeable future.

Astrocytomas and glioblastomas

Glioma brain tumours develop from glial cells which are non-neuronal cells of the central nervous system. Originally thought to be merely connective or supportive tissue to the neuronal cells, it has now been established that these cells play a vital role acting as 'partners' to their neuronal counterparts (Kettenmann et al., 2013). Astrocytes are a type of glial cell. Astrocytes have a multitude of functions ranging from maintenance of homeostatic factors linked to neuronal signalling, and encouraging growth events through the release of growth factors (Ransom & Ransom, 2012). Astrocytes are mainly inactive, however, becoming active and migratory in response to injury (Zhan et al., 2017). Astrocytes can develop into cancerous Astrocytoma tumours. These tumours can be graded based upon their characteristics. Less aggressive, benign tumours are grade I or II (lower grades) and the more aggressive, malignant tumours are graded III or IV (high grades) (Gupta & Dwivedi, 2017). Glioblastoma Multiforme (GBM) is the most malignant form of astrocytoma (Urbańska et al., 2014). GBMs are the most aggressive type of brain tumour. In comparison with lower-grade brain tumours, GBMs are easily identified as they are characterised by cell death regions (necrosis) and developing their own blood vessels to gain blood supply - enabling rapid growth and cell division - another feature of these high-grade tumours (Nørøxe et al., 2017). The main cause of tumour development is unknown, however, some GBMs may occur following a previous occurrence of a lower-grade astrocytoma caused by a malignant transformation – a secondary GBM. More commonly, 90% of GBMs are de novo (or primary) tumours (Song et al., 2013).

Despite years of research studying the pathology of GBMs, prognosis of the disease and its progression is still extremely poor. Symptoms of the disease result in reduced health-related quality of life (Dirven et al., 2014). Symptoms may vary dependent on the location of the tumour in the brain, but common observations among patients include the development of epilepsy, increased cranial pressure and cognitive deficits (Sizoo et al., 2010). Due to the characteristics of the tumour, there is currently no cure for the disease, however, there are several management options available to patients as a multi-therapeutic approach. Surgical tumour removal is the initial treatment and has proved to lead to a greater survival outcome than no treatment (Manrique-Guzmán et al., 2017). Chemotherapy using cytotoxic drugs such as temozolomide (TMZ) and radiotherapy targeting the abnormal tissue left around the tumour-removal site are palliative treatment options used following tumour removal (Zepecki et al., 2019). However, only around 2% of patients with GBMs survive for

three years with optimal combination treatment (Walid, 2008). Recurrence of these tumours is a common feature, and is largely due to the migratory characteristics of the GBM cells further invading the brain tissue, preventing complete tumour removal (Zhan et al., 2017). The survival rate for lower-graded brain gliomas is much greater in comparison, averaging at around seven years. Unlike GBMs, these tumours tend not to reoccur following surgical removal, due to the tumours not metastasising or migrating to other regions of the brain tissue (Claus et al., 2015). They have a slow proliferation, with tumours able to be detected and tracked before causing symptoms in the individual. Current tracking and imaging methods use magnetic resonance imaging (MRI) to track the tumour progression. This is preferable as it provides a non-invasive assessment of the character of the tumour (Villanueva-Meyer et al., 2017). The earliest symptoms detected are most commonly headaches due to the increased pressure within the cranium (hydrocephalus), often coupled with nausea and strabismus (eye misalignment) (Aiman & Rayi, 2020).

Glioblastoma cell migration

The morphological and pathological features of GBM further enable the migratory capabilities of the tumours. The centre of GBM tumours is hypoxic due to the rapid cell growth and division, increasing the oxygen diffusion distance into the tumour. It has been shown that the stress caused by the low oxygen levels within the tumour promotes the invasive characteristics of GBM. The morphological features resultant of the hypoxia are distinctive to GBM tumours (Monteiro et al., 2017). The first feature being necrotic foci, which are localised regions of cell death within the centre of tumours, producing holes where the GBM cells are unable to grow. The necrotic foci are then surrounded by psuedopalisades. These, also distinctive to GBM tumours, are elongated, stacked nuclei (Wippold et al., 2006) which are produced from cells migrating away from the hypoxic necrotic regions (Monteiro et al., 2017). Cells located further away from the tumour centre have access to more oxygen and are therefore able to multiply at a faster rate.

Following the induction of GBM migration due to hypoxic stress, the cells must acquire morphological alterations to migrate (Bronisz et al., 2020). There are two methods of cell migration involved within the single-cell invasion of oncogenic cells to other regions of the parenchyma. These are known as mesenchymal or 'path-generating' migration and amoeboid or 'path-finding' migration (Roussos et al., 2011). These two modes of migration are interchangeable and are dependent upon the surrounding brain tissue.

Initial acquisition of these migratory characteristics occurs through a process called 'epithelial-mesenchymal transition' (EMT). Through this process, cells are detached from their basement membrane and there is a decrease in the cell-cell adhesion (Iwadate, 2016). Changes within the cell morphology occur due to changes in gene expression to develop mesenchymal traits causing motility and invasiveness to develop as well as avoiding programmed cell death (a feature of healthy body cells) (Lu et al., 2020). These cells now appear long and thin, in contrast to the healthy astrocyte cells. Following this transition, the cell can now produce a long extension leading the directionality of the cell, extending within the direction of the movement. Enzymes are secreted from the polar front of the cell, to digest and degrade a path for the migrating cell. The cell migrates using proteins which adhere to the extracellular matrix (ECM) surrounding the brain tissue, driven by continuous reconstruction of the astrocyte cytoskeleton (Zhong et al., 2010). Particularly within GBMs, mesenchymal migration is linked to more aggressive tumours leading to a poor prognosis (Phillips et al., 2006).

Mesenchymal-amoeboid transition (MAT) is the mechanism in which cells of the mesenchymal subtype are transformed into amoeboidal migratory cells. This form of transition occurs at a more rapid rate in comparison with EMT as EMT requires far more extensive changes in gene expression compared to MAT. The reversal of this process,

amoeboid-mesenchymal transition (AMT) is also possible as the two processes are interchangeable. Changes to the migratory mode is due to the specific microenvironment of tumour (Panková et al., 2010). Amoeboid migration cell structure is more rounded in comparison to the mesenchymal migration structure. These cells have weaker bonds to the ECM. Amoeboidal migration does not degrade substances within the ECM as mesenchymal migration, and instead can adjust their shape to squeeze between cells within the ECM. Due to the lack of adhesion within the ECM, amoeboidal migration is much faster than mesenchymal migration (Talkenberger et al., 2017).

The effects of anti-migratory drugs

In this study, anti-migratory drugs were used to treat spheroids generated from the established glioma cell line U251 as carried out by Dr Brüning -Richardson for analysis. The drugs used were as follows: 6-bromo-indirubin-3'-oxime (Bio-indirubin/BIO), CCG 1423, Latrunculin A (LAT A) and Lithium Chloride (LiCl).

Bio-indirubin

BIO is a drug developed as a derivative of the compound indirubin. Indirubin is a chemical widely used in traditional Chinese medicine, initially obtained from the Indigo Plant (Indigofera tinctoria) and is now synthesised synthetically (Blažević et al., 2015).

Activity of BIO has been shown to inhibit Glycogen synthase kinase-3β (GSK-3β), an enzyme involved, among others, in the regulation of cell migration (Meijer et al., 2003). GSK-3β interacts with the protein β-catenin (Nager et al., 2012). β-catenin plays a role in the regulation of cell-cell adhesion during cell migration (Amin & Vincan, 2012). Briefly, GSK-3β interaction causes an accumulation of β-catenin in the cell cytosol (Nakada et al., 2011). β-catenin is transported to the cell nucleus, where it interacts with the DNA, increasing GBM cell migration (McCord et al., 2017). BIO interrupts this pathway through the inhibition of GSK-3β, preventing the downstream interaction with β-catenin.

It is worth mentioning that GSK-3β has multiple intracellular targets as indicated in studies by Brüning-Richardson et al. (2018) and Sun et al. (2009). Previous studies into the effect of BIO on GSK-3β have indicated that decreasing the presence of GSK-3β using other compound substances, in some instances, does not completely inhibit cell migration and invasion. The conflicting evidence indicates that BIO may target other signalling molecules within the migration mechanism cascades by its mode of action (Braig et al., 2013).

CCG-1423

The CCG-1423 inhibitor can inhibit RhoA/C-enzyme, responsible for folding the DNA to effect gene expression relating to cell migration (Symons & Segall, 2009). Expression of RhoA and RhoC is increased within oncogenic cells (Croft & Olson, 2011). This allows remodelling of the cell structure to happen at a rapid rate (Parri & Chiarugi, 2010). CCG-1423 specifically targets Megakaryoblastic leukaemia 1 (MKL1) signalling proteins (Ketchen, 2019) in GBM cells. In untreated GBM cells, migration is mediated via Rho signalling of serum response factor (SRF) proteins and co-activator MKL1 (Evelyn et al., 2010). Studies within endothelial cells (EC) have shown that SRF regulate genes which act upon the cell structure. MKL1 stimulates SRF's ability to affect gene expression through binding together to form a complex. In vitro studies have demonstrated that inactivation of MKL or SRF genes prevent migration in human EC. Through inhibition of MKL1, CCG-1423 can prevent the formation of the MKL-SRF complex, leading to the anti-migratory effects (Gau et al., 2017).

Latrunculin A

Latrunculin A (LAT A) is a compound originally isolated from the Negombata magnifica or Red Sea Sponge (Yarmola et al., 2000). LAT A is able to bind

with actin monomers (proteins that are responsible for the cell's structure) to disrupt the polymerisation (combining) of these monomers, preventing cell migration (Coué et al., 1987). This occurs through LAT A molecules sequestering G-actin monomers. LAT A has shown to be very efficient in the treatment of other types of cancers (Gandalovičová et al., 2017). LAT A has been found to decrease the invasiveness of GBM cells within tumour spheroids through the reduction of actin filaments within the migrating cell (Ivkovic et al., 2012).

Lithium chloride

Lithium chloride (LiCl) is also a drug recognised for its therapeutic abilities in oncogenic cells surrounding the inhibition of GSK-3β. Therefore, downstream effects of GSK-3β inhibition would also prevent β-catenin mediated gene expression, as seen with BIO. Extensive research into the effects of LiCl upon colorectal cancer has found it is able to induce cell death within these cells, therefore increasing survival rates within individuals with the disease (Li et al., 2014). A study from Nowicki et al. (2008), indicated the anti-migrastatic ability of LiCl within two different glioma cell lines in comparison with other lithium and chlorine compounds. This study also highlighted that inhibition of GSK-3β plays a role within inhibiting the migratory characteristics of these glioma cells. The mechanism of the observed inhibition of GSK-3β and LiCl is unknown, however, two mechanisms are suggested. The first is that the Li^+ acts as a competitive inhibitor to Mg^{2+} for the GSK-3β binding site. The second suggestion is that Li^+ prevents potassium

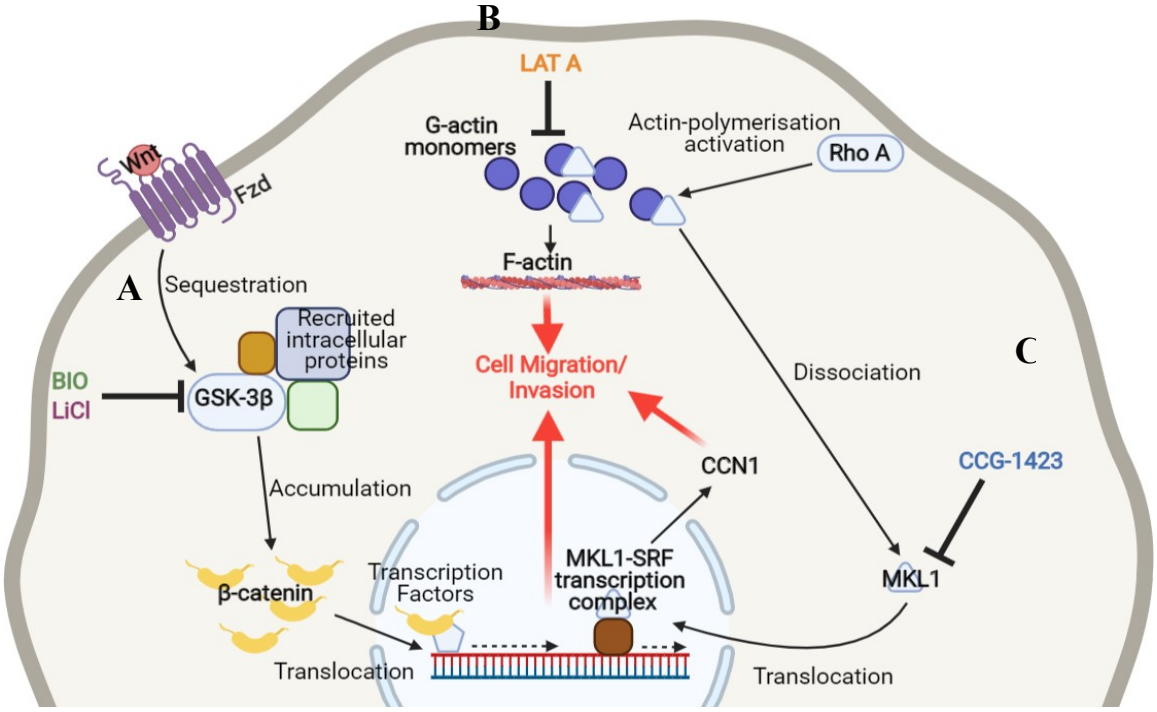

Figure 1: Simplified diagram depicting the intracellular targets of the anti-migratory drugs on GBM used within this study: BIO = 6-bromo-indirubin-3'-oxime, LiCl = Lithium Chloride, LAT A = Latrunculin A and CCG-1423. A) inhibition of GSK-3β by BIO and LiCl to prevent cell migration. Under normal conditions, GSK-3β is signalled by cellular proteins to cause the accumulation of β-catenin within the cytosol. This causes its transportation into the nucleus. In the nucleus, it binds with proteins to alter the DNA expression and certain genes, which increase cell invasion. B) LAT A forms a complex with g-actin monomers to prevent migration. Polymerisation of g-actin monomers causes the rearrangement of the cytoskeleton causing the cells to acquire invasive and migratory effects. C) CCG-1423 inhibits MKL1 proteins to exert its effects. The MKL1 proteins are transported to the nucleus via transport proteins. MKL1 forms a transcription complex with SRF, causing the proteins associated with cell causing the invasive cell characteristics. (Created with BioRender.com)

deprivation of GSK-3β causing it to become inhibited (Keamer et al., 2012).

Figure 1 shows how each of the anti-migratory drugs act upon their intracellular targets, and how these targets work to cause GBM cell migration.

Aims and objectives

The aims of this study are to investigate the effect of the anti-migratory drugs on GBM tumour spheroids to assess the potential for possible combination therapies for GBM treatment in the future.
This will be achieved through analysing scanned, immunohistochemistry (IHC) sections of the tumour spheroids established from the U251 glioma cell line – generated prior to this study. To assess the effect of these inhibitors on migration, the migration distances of migrating GBM cells from the tumour spheroid will be measured using the computational software, QuPath. The 'cell circularity index' of the migrating cells in comparison with the 'cell circularity index' of the static cells within the tumour will also be analysed in QuPath. The 'cell circularity index' should aid in understanding the mode of migration of the tumour cells, and to see how the treatments may have altered this. The spheroid morphologies from each treatment will also be discussed, briefly indicating GBM tumour features and how these may have been altered across the treatments. Through comparison of the treated spheroids against an untreated control, the efficacy of the anti-migratory drugs was determined. Statistical analysis of the data obtained was carried out using SPSS to indicate significance within the study.

Methods and materials

2.1 Spheroid generation

Spheroids were prepared by Dr Anke Brüning-Richardson prior to the analysis carried out in this study. The method for the spheroid generation was as prepared in Rohwedder et al., 2021 –(manuscript in preparation). Briefly, the glioma cell line U251 was grown, as previously described, in vitro (Cheng et al., 2015). Spheroids were generated from the cells in low adherent 96-well plates (Nunc, UK), as previously described (Cheng et al., 2015), embedded in collagen and treated with three inhibitors at predetermined anti-migratory concentrations including 6-bromo-indirubin-3'-oxime (5 mM) (Selleckchem), latrunculin A (1 mM) (latA, Tocris), and CCG-1423 (500 nM) (Tocris) and allowed to migrate into the collagen over 72 hours. After completion of the experiment the whole collagen plugs containing the spheroids and migrating cells were prepared for immunohistochemistry (IHC). Paraffin-embedded spheroids and migratory cells were serially sectioned at 5 μM using Haemotoxylin and Eosin staining for reconstruction of the whole spheroid and surrounding migratory rim. Slides were scanned using Aperio digital scanners (Leica Biosystems) at 20x magnification at the University of Leeds.

Cell migration distance analysis

All spheroid section images were analysed for both sets of analysis to increase the significance level of the results due to a large sample size. For each condition, Control – 49 GBM slides were annotated, and 3104 cell measurements were recorded, BIO - 66 slides annotated and 736 cell measurements, CCG-1423 – 62 slides and 628 cell measurements, LAT A – 36 slides and 409 cell measurements and LiCl – 79 slides and 2476 cell measurements. The spheroid slides were uploaded as images onto the computer software QuPath (Bankhead et al., 2017) for analysis. The spheroids were highlighted using the 'Shape Annotation Tool'. 'Positive cell detection' was then run to indicate positive and negative cells within the sections (Analyse > Cell detection > Positive cell detection). For the Haematoxylin and Eosin stain, positive cells are based on 'the score compartment value' of each stained nucleus. This is assessed through comparison of the value of each eosin-stained nucleus against the mean average value of the eosin stain on the nuclei, of the detected cells The single threshold value was set to 0.1. Cells then appeared

either red or blue denoting positive and negative cells, respectively. Negative cells were not included in the measurements.

Using the line annotation tool, measurements were obtained from the perimeter of the tumour spheroid to the perimeter of each identified migrated cell. This was repeated for each image section for each spheroid treatment and the annotation measurement data was exported (Measure > Show annotation measurements) and compiled using Microsoft Excel separately for each spheroid.

Figure 2 shows a representative example of an annotated slide from the control spheroid. The compiled cell migration data for each spheroid was then analysed in SPSS (Version 26). Descriptive statistics were obtained for each spheroid. The normality for each of the spheroid measurements was analysed, and this indicated a Kruskal-Wallis to compare the data. Following this, a post-hoc, pairwise analysis was further carrier out to indicate significant differences between each pair of spheroids.

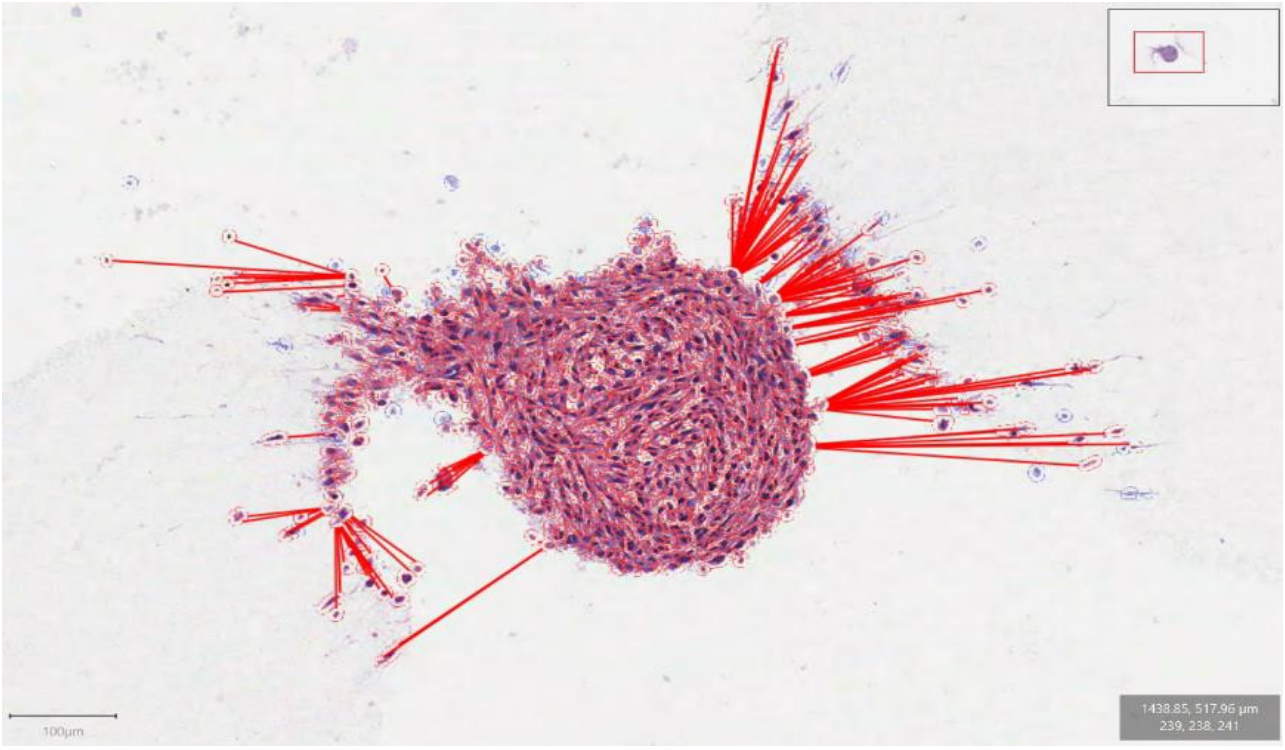

Figure 2: Spheroid from the untreated control with at x10 magnification, cell migration distances measured using QuPath. Positive cells (as indicated following the positive cell detection) are highlighted red. Negative cells, indicated by the blue borders, have been excluded from the measurements. The thick red lines, produced using the 'Line Annotation Tool', produce measurements based upon the length of the line from the perimeter of the migrated cell to the perimeter of the tumour cell. These measurements were exported from 'Measure' > 'Show annotation measurements'

Cell circularity analysis

The spheroid sections were analysed using QuPath. For each spheroid two different cell detections were run, depicted in Figure 3.

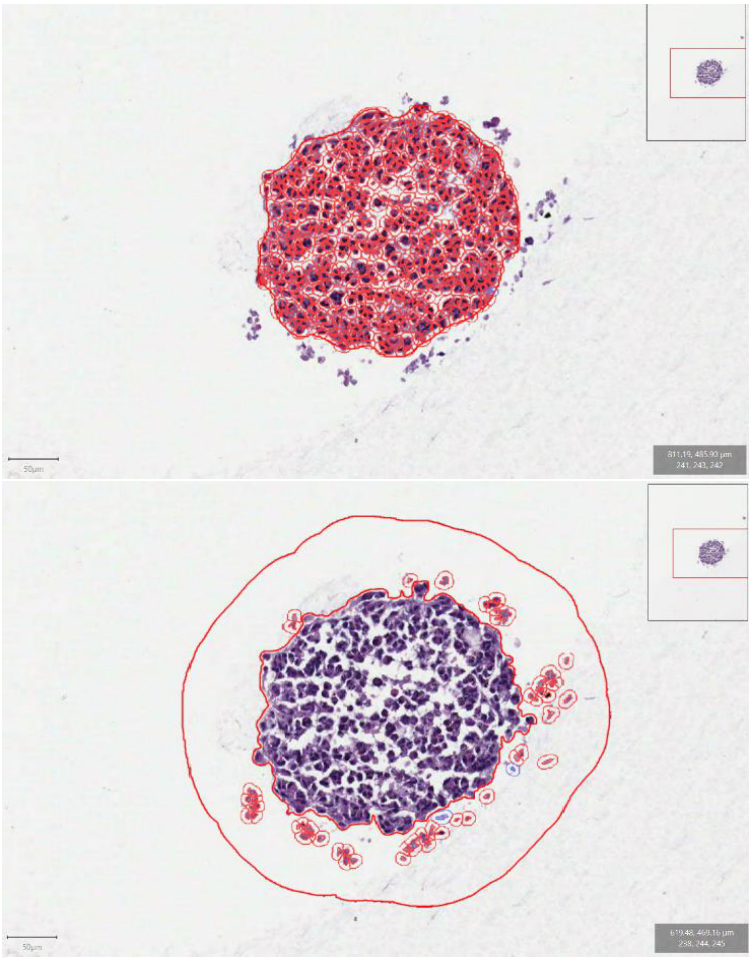

Figure 3: Positive cell detection of tumour spheroid (top) and positive cell detection from the perimeter of the tumour into the surrounding matrix (bottom) obtained from QuPath at x10 magnification

Using the 'Wand' annotation tool, the cells of only the spheroid tumour were highlighted and positive cell detection, again at the 0.1 single threshold value, were detected. The detection measurements were exported to Microsoft Excel to be sorted so negative cell detections for each slide were removed. The tumour cell detections were then removed from the slide. This method was repeated, but instead of analysing cells within the spheroid, the 'Wand' annotation tool was used to highlight migrated cells from the perimeter of the spheroid. Positive cell detection was run and the detection measurements were exported onto a separate spreadsheet. This data was analysed in SPSS. This was carried out for each of the different cell treatments and control. Using SPSS, descriptive statistics were obtained to find the mean values and SEMs for each treatment data set for the migration and tumour cell circularity separately. Following this, a normality test indicated a non-parametric, Mann-Whitney analysis was carried out analysing the circularity data between the tumour cells and the migrated cells for each treatment, producing five significance values. Then, differences between the migrated cell circularity of each of the five different spheroids were analysed using a Kruskal-Wallis test, followed by a post-hoc for direct pairwise comparison.

Results

Cell migration

The descriptive statistics were generated with the software application SPSS (Appendix 1). The mean migration distances varied among the spheroid treatments as shown in Figure 4. On average, the longest cell migration distance was recorded for the control spheroid with a mean of 102.73µm (SEM ± 1.70). For the treatments, the mean migration measurements were as follows: Bioindirubin at 32.04µm (SEM ± 1.45), CCG-1423 at 40.54µm (SEM ± 1.73), Latrunculin A at 16.95µm (SEM ± 0.65) and lithium chloride at 41.07µm (SEM ± 0.72).

To analyse the significance of the Kruskal-Wallis tests for cell migration distances, the hypothesis and null hypothesis were as follows:

H1 – There is a significant difference between the cell migration distances between the control spheroids and each of the treated spheroids.

H0 – There is no significant difference between the cell migration distances between the control spheroids and each of the treated spheroids.

The Kruskal-Wallis test indicated there was a significant difference between the different spheroid

treatments (sig. = 0.000) and therefore the H0 was rejected (Appendix 2). The post-hoc pairwise comparisons of the spheroid treatments (Appendix 3) indicated that all bar one of the comparisons showed significant differences – pairwise comparison of Bio-indirubin and the CCG inhibitor (sig. = 0.130).

Therefore, for all the pairwise comparisons, the hypothesis (H1) can be accepted – indicating that there is a difference between the migration measurements of each tumour spheroids and control spheroid.

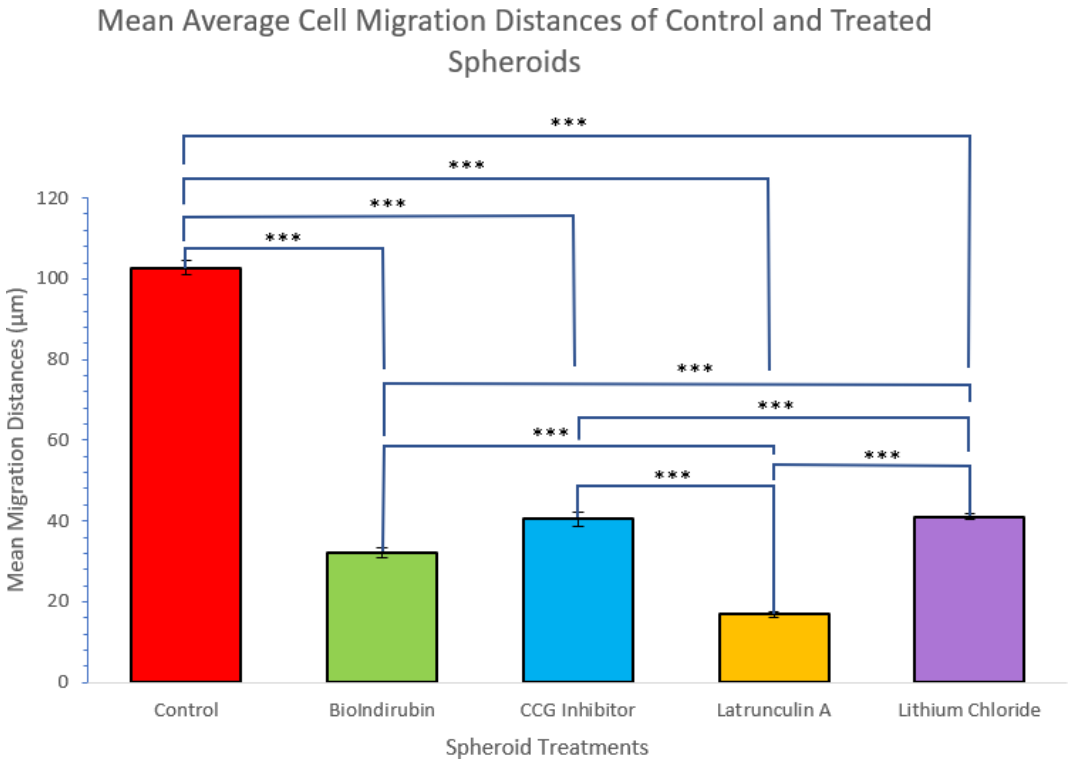

Figure 4: Mean average cell migration distances across each of the spheroid treatments. Error bars indicating the standard error of the mean for each treatment. Asterisk brackets indicate statistical significance obtained from the pairwise Kruskal-Wallis Comparison, * - P ⩽ 0.001**

Cell circularity

Cell circularity measurements in QuPath were defined as $4\pi A/P2$ where A = Area and P = Perimeter, producing values from 0 to 1 (with 1 indicating perfect circularity).

Figure 5 shows the means cell circularity values of both the migrated cells and cells within the tumour spheroid for each spheroid treatment and control (see methods in Figure 3 for measurements) obtained from the descriptive statistics analysis from SPSS (Appendix 4). Error bars indicate the standard deviation.

To analyse the significance values from the Mann-Whitney analysis of the cell circularity between the migrated cells and the tumour spheroid cells, the hypothesis and null hypothesis were as follows:
H1 – There is a significant difference between the cell circularity of the migrated cells and the cells found within the tumour spheroid.
H0 – There is no significant difference between the cell circularity of the migrated cells and the cells found within the tumour spheroid.

The Mann-Whitney SPSS tests indicated that there were significant differences between the circularity of the migrated cells and tumour spheroid cells for each individual treatment (see Appendix 5). This indicated the H0 could be rejected and that the H1 was true, indicating there were significant differences between the migrated cell circularity and the tumour cell circularity.

To analyse the significance of the Kruskal-Wallis tests for cell circularity, the hypothesis and null hypothesis were as follows:

H1 – There is a significant difference between the cell circularity measurements of the migrated cells from the spheroid treatments.

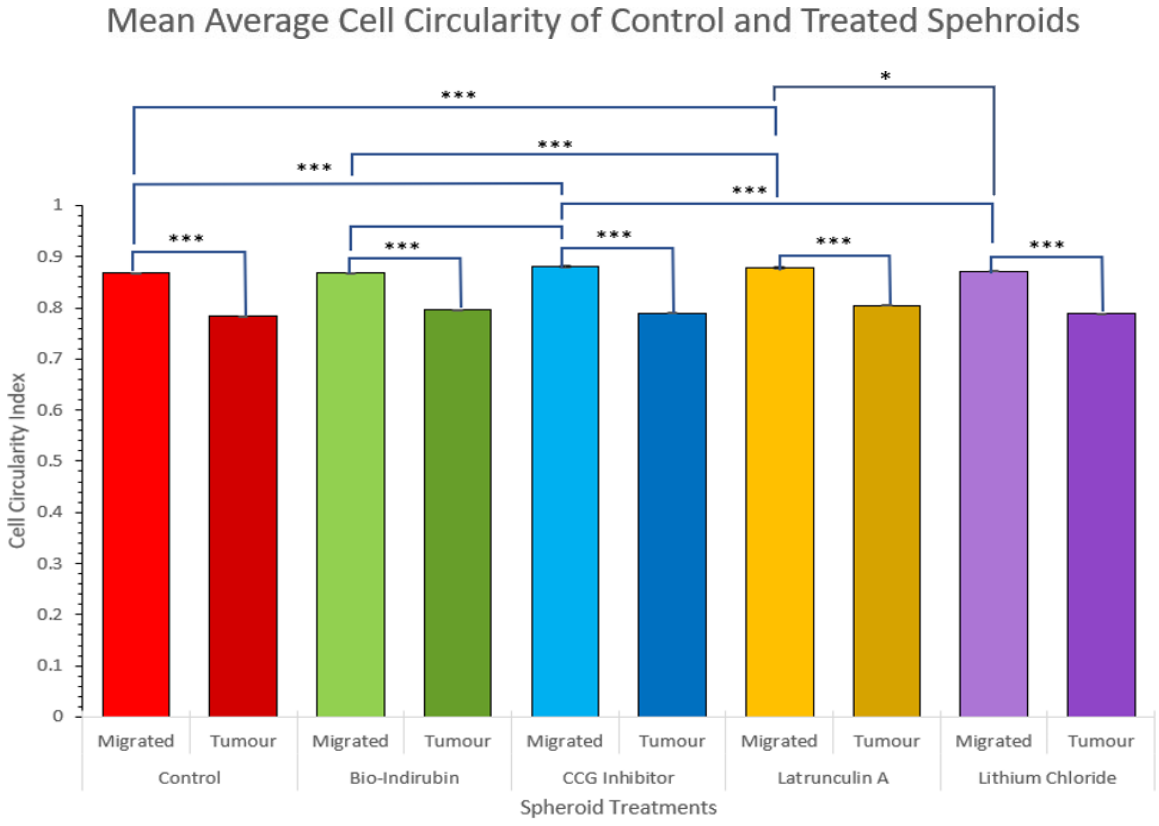

Figure 5: Mean average cell circularity for the control and treated spheroids. Migrated cell circularity is indicated on the left bar and tumour cell circularity is indicated by the right bar for each treatment. Error bars indicate the standard error of the mean for each of the spheroid measurements. Asterisk brackets indicate statistical significance indicated by the Mann-Whitney and pairwise Kruskal-Wallis Comparison, * - P ⩽ 0.05, * - P ⩽ 0.001**

H0 – There is no significant difference between the cell circularity measurements of the migrated cells from the spheroid treatments.

The Kruskal-Wallis test indicated that there was a significant difference between the migrated cell circularity among the five treatments. Therefore, the H0 could be rejected and the H1 was accepted. The post-hoc analysis indicated the differences through pairwise comparisons of the treatments. There were significant differences between five of the pairwise comparisons (highlighted in Appendix 6). These were as follows; Bio-indirubin and Latrunculin A (sig = 0.001), Bio-indirubin and CCG inhibitor (sig = 0.000), Control and Latrunculin A (sig = 0.001), Control and CCG inhibitor (sig = 0.000), Lithium Chloride and CCG inhibitor (sig = 0.000) and Lithium Chloride and Latrunculin A (sig = 0.016).

Cell morphology

The observations of the GBM spheroid sections indicate many of the features that are commonly seen within GBMs in vivo. Features such as cell migration and the changes in the morphology of these migrating cells can be seen. Hypoxic regions could also be observed, however, it is worth noting that, to achieve conclusive evidence of this, further staining would be required. Figure 6 highlights the morphological features of the control GBM tumour spheroid sections. In comparison with the other GBM tumour treatments, it is evident there is far more cell migration from the tumour spheroid. Areas where the cell migration appear to be most prevalent are highlighted within the blue regions on the images. Within these regions, these migrated cells appear more elongated as they migrate further from the spheroid. his showing the change of morphology as the cell appears more elongated as they migrate further away.

Control Spheroid

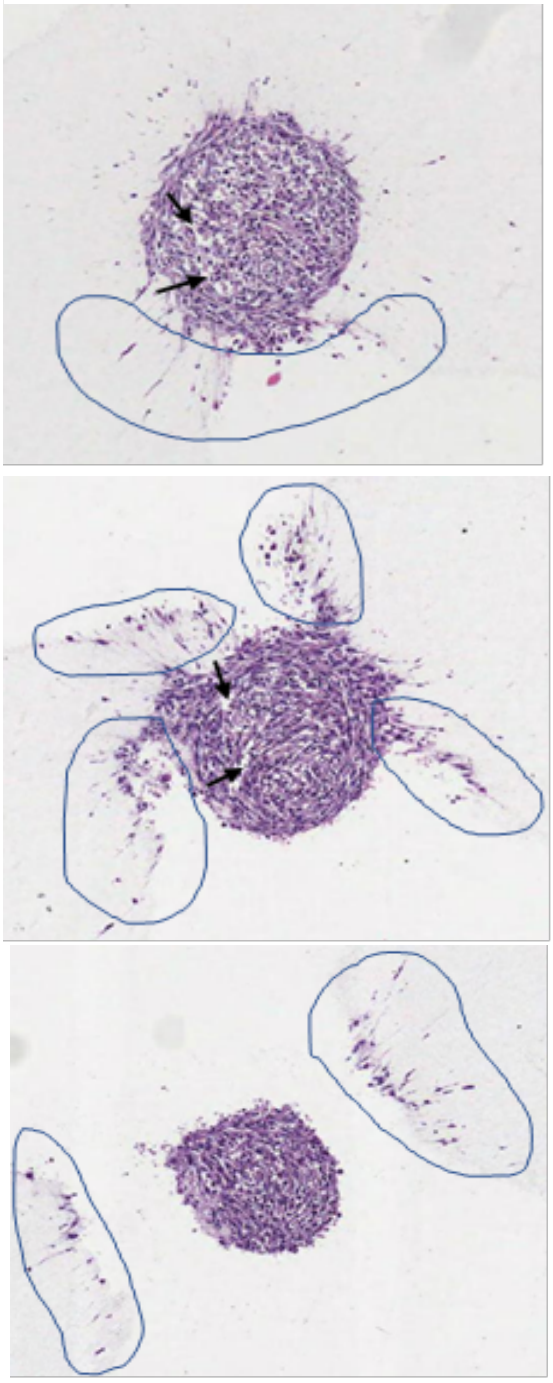

Figure 6: Control GBM spheroid images at x10 magnification, contained within a collagen matrix. Slides obtained using immunohistochemistry techniques stained using eosin and haematoxylin. Black arrows indicate the appearance of necrotic loci, and the blue rings indicate the regions of significant cell migration

This can be seen in Figure 7, cells closer to the spheroid border – indicated by the yellow line, are more spherical compared to the cells further away. There also appear to be several small necrotic regions around the centre of the GBM tumours, indicated by black arrows in Figure 6. These tumour spheroids generally appear very spherical and rounded.

Figure 8 shows further magnified images of specific migrating cells at x60 magnification. The image on the left was taken close to the edge of the tumour border and appears spherical and rounded. In the right image, taken further away from the spheroid edge, the cell appears elongated, and the cytoplasm is stretched.

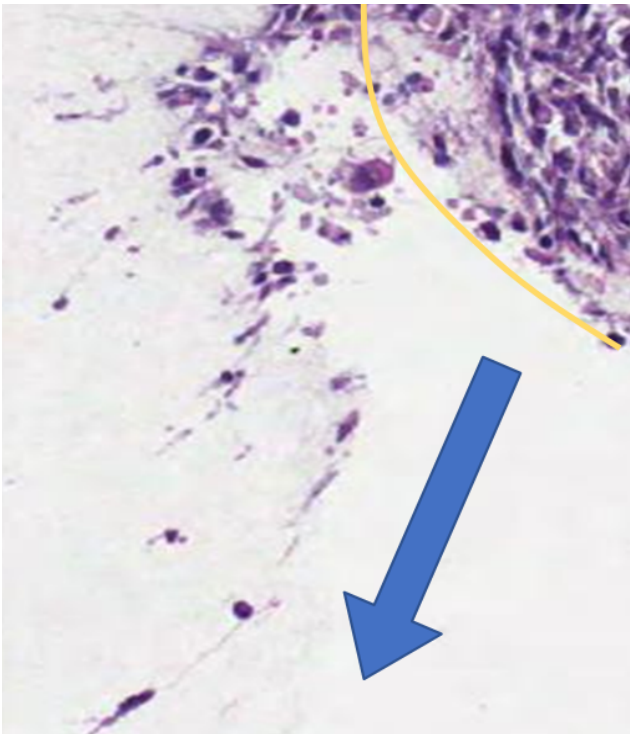

Figure 7: Control GBM spheroid section at x15 magnification. Spheroid perimeter is indicated by the yellow border. The blue arrow indicates the direction of the migrating cells. Cells become more elongated as they move further away from the tumour spheroid border

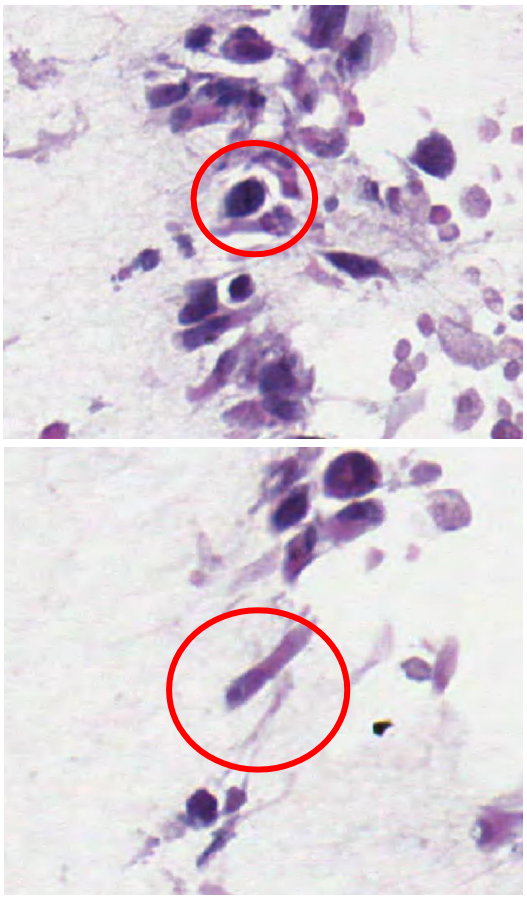

Figure 8: Control spheroid migrating cells at x60 magnification. A single cell in each image is indicated by the red circle. The top cell image was taken close to the border of the tumour spheroid and the bottom cell image was taken further into the collagen matrix, away from the spheroid

Figure 9 indicates the morphological features of the BIO-treated GBM spheroid tumours. As with Figure 6, regions of cell migration are indicated by the blue ring. There is less migration with these cells, compared to the control and there also appear to be fewer, smaller necrotic loci. The spheroid shapes also are less rounded than the spheroids of other treatments.

Bio-indirubin

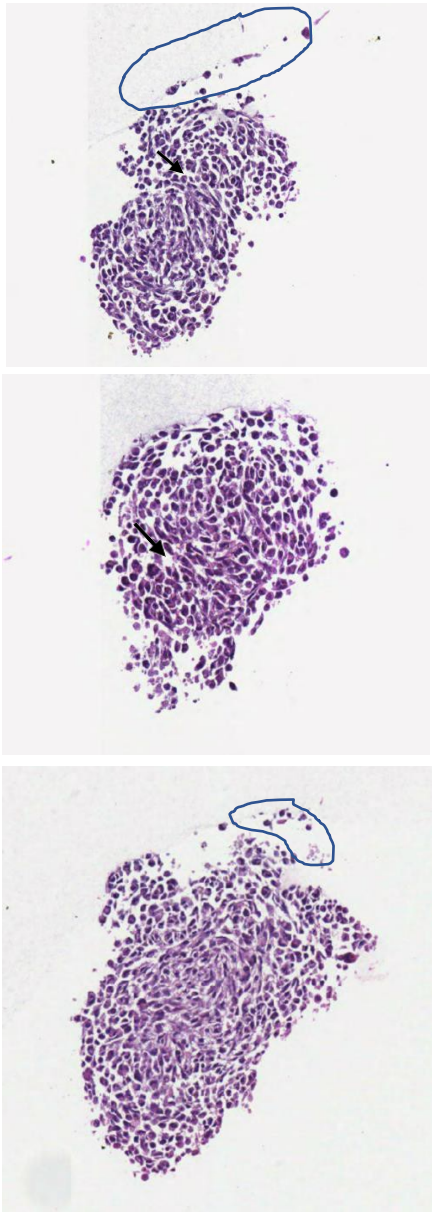

Figure 9: Bio-indirubin-treated GBM spheroid images at x10 magnification, contained within a collagen matrix. Slides obtained using immunohistochemistry techniques stained using eosin and haematoxylin. Black arrows indicate the appearance of necrotic loci, and the blue rings indicate the regions of significant cell migration

Figure 10 shows three spheroid slides treated with CCG-1423. There is far less cell migration in comparison with the control spheroid, as indicated in Figure 6, as there only appears to be one region of migrating cells shown in the three images. However, there appear to be many regions of small necrotic loci in comparison to the control and the other treatments. The spheroids generally appear very spherical.

CCG-1423

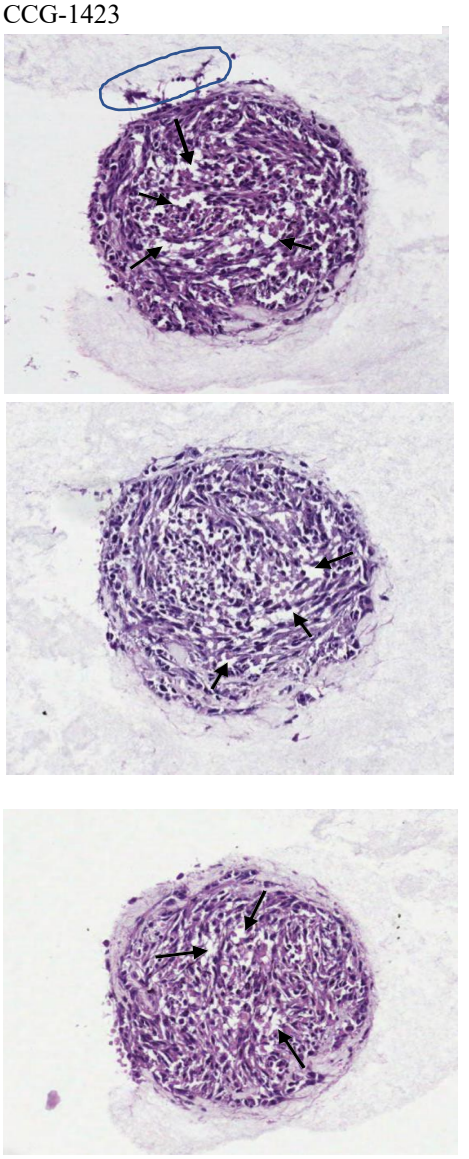

Figure 10: CCG inhibitor-treated GBM spheroid images at x10 magnification, contained within a collagen matrix. Slides obtained using immunohistochemistry techniques stained using eosin and haematoxylin. Black arrows indicate the appearance of necrotic loci, and the blue rings indicate the regions of significant cell migration

The LAT A-treated tumour spheroid shown in Figure 11 shows that there is minimal cell migration as indicated by the small area of the blue rings. The black arrows also indicate many necrotic regions within the centre of the tumour spheroid. These tumours are generally spherical.

Latrunculin A

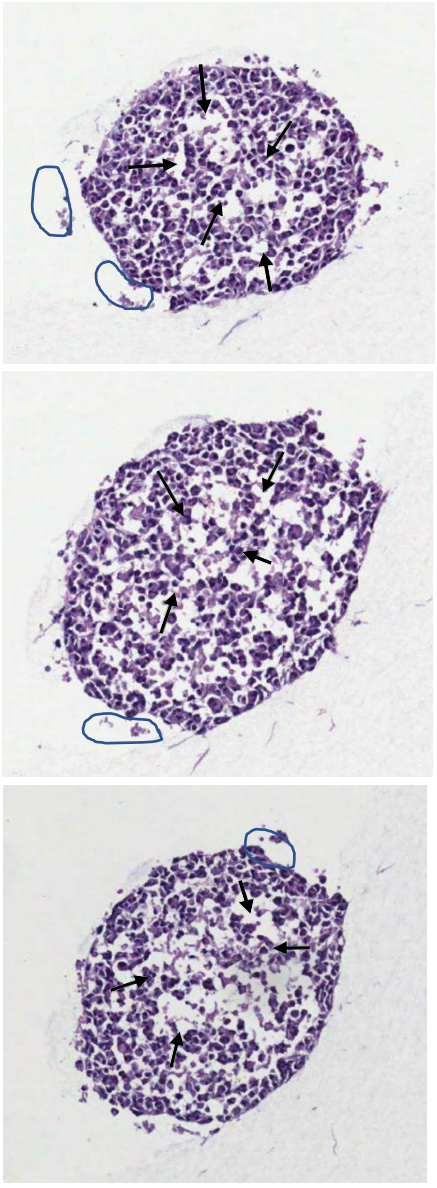

Figure 11: Latrunculin A-treated GBM spheroid images at x10 magnification, contained within a collagen matrix. Slides obtained using immunohistochemistry techniques stained using eosin and haematoxylin. Black arrows indicate arrows the appearance of necrotic loci, and the blue rings indicate the regions of significant cell migration

Figure 12 shows the morphology of the LiCl-treated GBM spheroids. There appear to be multiple, large necrotic regions within the centre of the spheroids, as indicated by the black arrows on the diagrams. The blue rings indicate there are large regions of cell migration.

Lithium Chloride

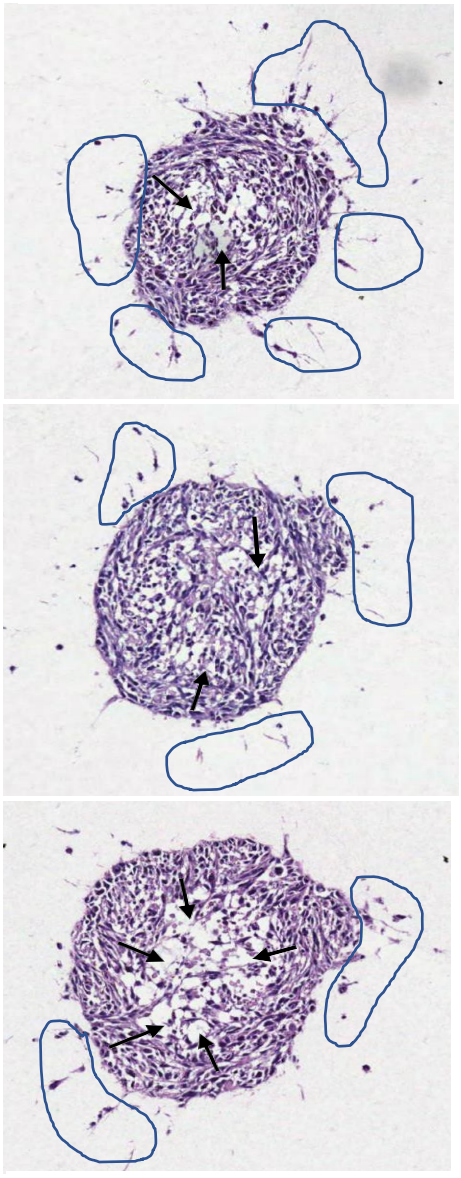

Figure 12: Lithium Chloride-treated GBM spheroid images at x10 magnification, contained within a collagen matrix. Slides obtained using immunohistochemistry techniques stained using eosin and haematoxylin. Black arrows indicate the appearance of necrotic loci, and the blue rings indicate the regions of significant cell migration

Figure 13 is a section taken from a LiCl-treated spheroid. Similarly to Figure 7, it can be seen that migrating cells are more spherical close to the border of the spheroid. As they migrate further away, these cells become more elongated (this indicated by the arrow on Figure 13).

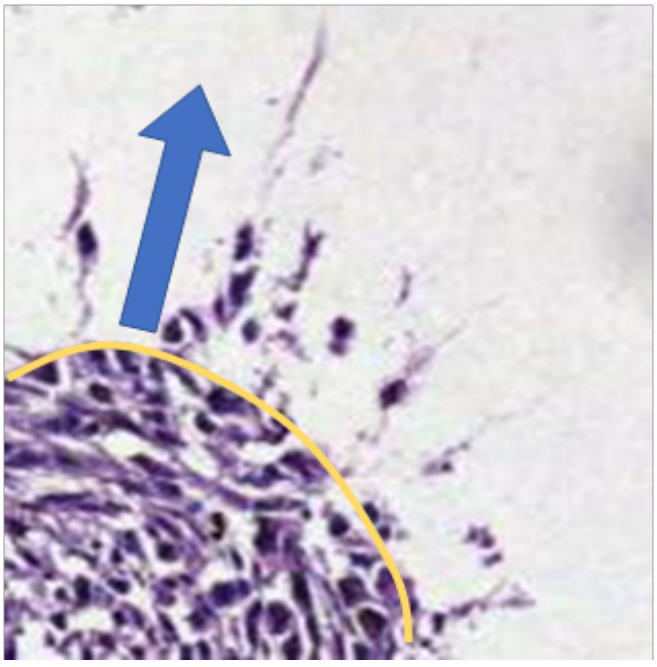

Figure 13: GBM spheroid section. The spheroid perimeter is indicated by the yellow border. The blue arrow indicates the direction of the migrating cells. Cells become more elongated as they move further away from the tumour spheroid border

Figure 14 further highlights the changing of cell morphology during cell migration, focusing on two cells at x60 magnification. The image on the left shows a migrating cell close to the perimeter of the spheroid, with the cytoplasm appearing more spherical and rounded. The image on the right shows the migrating cell further away from the tumour.

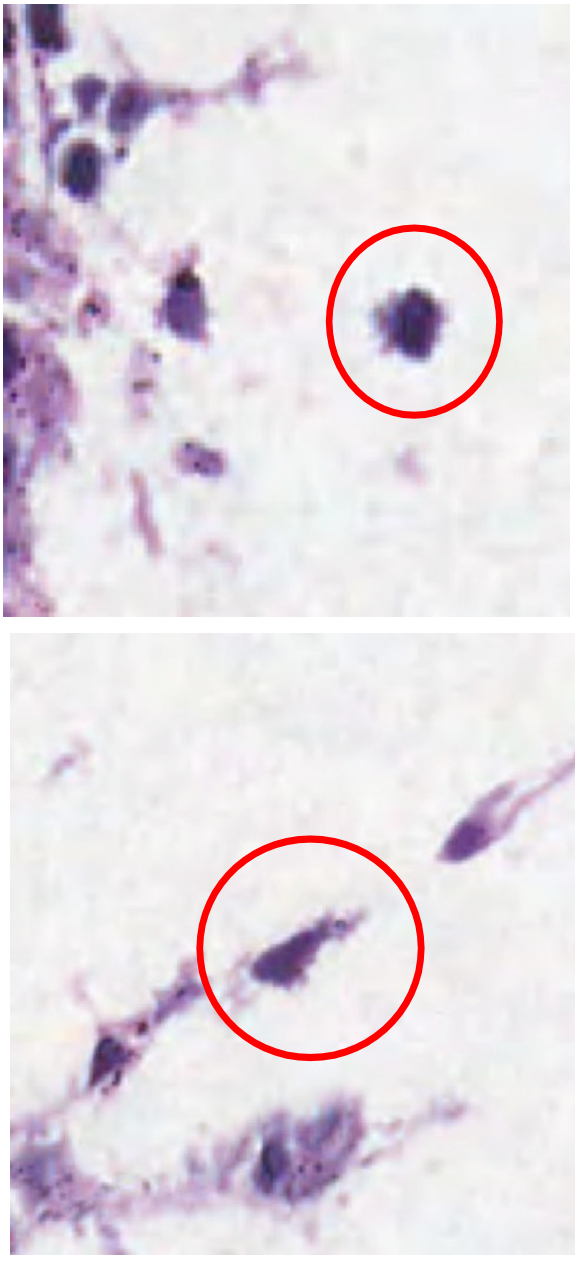

Figure 14: Lithium Chloride-treated spheroid migrating cells at x60 magnification. A single cell in each image is indicated by the red circle. The left cell was taken close to the border of the tumour spheroid and the right cell was taken further into the collagen matrix, away from the spheroid

Discussion

Overview

High-grade gliomas, in particular GBM, have an extremely poor prognosis with an average of 15 months survival (Naydenov et al., 2011). Tumour resection continues to prove relatively ineffective for tumours of this type, due to their highly invasive behaviour, leading to secondary tumour development within a new region of the brain tissue (Claus et al., 2015). Combined treatment regimens of chemotherapy and radiotherapy are still used to treat GBM (Zepecki et al., 2019), however, prognosis using these treatments remains poor. Novel treatments aim to improve the survival rates of GBM, through preventing the invasion of GBM into the surrounding tissue to enhance the treatment options for the patient. These treatments complementary to radiotherapy and chemotherapy aim to tackle the aggressive characteristics of these tumours, targeting the high rates of cell migration, and improve overall prognosis for patients.
Overall, the data obtained from the statistical analysis clearly indicates that the compounds had an effect on reducing the migration of cells from the tumour spheroid. This is shown in Figure 4, as, not only is there a significant difference within the mean cell migration distances between the control spheroid and each of the anti-migratory drugs used within the study, but statistical significant differences between each of the pairwise comparison were also observed – as indicated

Potential adjustments to the cell circularity index study

There were also significant differences between the 'cell circularity index' between the migrated cells and the cells within the tumour spheroid for each individual treatment. However, the data does not represent what would be expected for the mode of migration within the tumour cells. The data shown in Figure 5 shows that for each spheroid treatment, the migrated cells have a higher 'cell circularity index' on average, than that of the cells in the tumour spheroid. This means that these migrating cells have a more 'rounded' cytoplasm in comparison to the tumour spheroid cells. Within GBM cells, mesenchymal migration is the mode of migration generally associated with this glioma type due to its aggressive invasive characteristics (Phillips et al., 2006). Mesenchymal cells characteristically appear elongated due to actin polymerisation within the cytoplasm pushing the cell membrane at the leading edge to migrate (Zhong et al., 2010). An example of a cell migrating with a mesenchymal morphology can be seen in the bottom image on Figures 8 and 14. Due to this change in morphology, it would therefore be expected that, particularly in the control, the migrated 'cell circularity index' would be lower than that of the cells within the tumour due to the elongated cytoplasm observed in these cells.

Control spheroid shows classical features of GBM tumours

The control morphological analysis, shown in Figure 6, clearly highlights the common pathological features of GBM tumours as described. The large regions of cell migration show evidence of mesenchymal migration as the cells undergo EMT (Zhong et al., 2010). Cells detaching from the spheroid border appear more spherical. Following this, the cell cytoplasm appears to become more elongated as they migrate further away from the spheroid – a common feature of mesenchymal cells (Figure 7). Necrotic regions due to hypoxia within these tumours appear to be observed in Figure 6, however, further evidence would be required to confirm this, as mentioned. Use of stains such as pimonidazole and EF5 have been identified as effective stains for IHC detection of hypoxia in tumours (Russell et al., 2009), and would help to provide quantitative evidence to confirm the presence of necrotic regions in the GBM slides. Although these regions were observed, they were, however, not as prominent in comparison with other cell treatments. The data obtained from the treatments in comparison to the drug treated spheroids clearly shows that these treatments have an effect on reducing the cell migration through interaction with molecular targets.

Potential for further development of BIO for the treatment of GBM cell migration

BIO showed particularly promising results within this study. There was a clear significant difference between the migration distances of the BIO-treated spheroid and the control spheroid. Morphological analysis showed these spheroids were less spherical compared to the other spheroid treatments. As the migration distances were significantly shorter than to that of the control, less evidence of mesenchymal migration could be seen, however, migrating cells with an elongated cytoplasm could still be seen (as indicated with the top image of Figure 9).

BIO has been shown to target GSK-3β (Meijer et al., 2003) and has been proven effective in treating many different forms of cancer, such as breast cancer (Braig et al., 2013) and melanoma (Liu et al., 2011). GSK-3β has been shown to interact with the signalling of multiple molecules in relation to GBM cell migration, as previously mentioned. The main targets of GSK-3β that have been identified as influencing cell migration are β-catenin (Shevchenko et al., 2019) and the Rho-family GTP-ases, Rac and Rho (Sun et al., 2009). The data obtained from this study clearly indicates the efficacy of BIO in vitro for the targeting of migration and invasion within GBM. This has also been supported in prior studies such as Williams et al. (2011). Due to the variety of GSK-3β molecular interactions, the enzyme also has been shown to have a role in the development of other aspects and forms of cancer. As BIO has proven effective within the treatment of other cancers, such as melanoma (Liu et al., 2011) and prostate (Zhang et al., 2017), there are further studies into the in vivo activity.

There are few studies into the specific in vivo activity of BIO within GBM cells. A study from Williams et al. (2011) investigates the effect of BIO on β-catenin in vitro also in the U251 cell line. The data from the in vitro study showed BIO was able to decrease cell migration as expected. The in vivo experiments within this study focused on a derivative of BIO, however, being 6-bromo-indirubin acetoxime (BIA). This examined the effects of BIA upon a human glioma-derived neurosphere line, GBM9, in a mouse model. The in vivo study showed that there was a decrease in cell migration with treatment of BIA in mice models. It is also worth noting that there was a five-fold decrease in tumour volume following BIA treatment within this study. A study from Meijer et al. (2003), examined the effects of indirubins as selective GSK-3β inhibitors. Due to the promising results obtained over a multitude of studies into the effects of BIO upon various types of cancer, further studies into the in vivo activity of BIO on GBM should be carried out. This will allow for further assessment of the therapeutic potential of the drug, and thus, be able to identify the potential of combination therapies in the future. BIO has not yet been used in clinical studies. As BIO is a derivative of indirubin, further changes to the structure of BIO may improve the pharmacodynamic profile, like BIA. This is due to the low solubility and hydrophobic properties required of these drugs, to interact with GSK-3β (Meijer et al., 2003).

CCG-1423 analogue provides evidence for potential combination treatment for cell migration inhibition

CCG-1423 also showed promising results within this study. There was a significant difference between the control spheroid and the CCG inhibitor in the cell migration distances from the spheroid, although it produced one of the longer mean migration distances within the study. The morphological assessment within these studies showed that there were few, small hypoxic regions seen in the IHC slides, and perhaps as a result, had led to the lower instances of cell migration.

As previously mentioned, CCG-1423 exerts inhibitory effects upon Rho-stimulated gene transcription. In terms of migration, Rho aids the regulation of amoeboid migration within GBM, which is commonly upregulated within these cells (Evelyn et al., 2007). The effects of CCG-1423 were discussed in an in-depth thesis from Ketchen (2019) regarding the effects of the inhibitor in vitro and in

vivo. A similar assay to those used in this study was carried out on the U251 cell line, looking at similar inhibitors including CCG-1423. The data obtained shows that the migration distances of the cell line treated with CCG-1423 only just managed to reach significance (P=0.03) when compared to the control. The study also focused on the presence of lamellipodia – a feature commonly linked to mesenchymal migration in GBM cells, and filopodia, thin actin projections from the edge of the cytoplasm (Panková et al., 2010). It was found that treatment with CCG-1423, reduced the formation of lamellipodia and an increase the filopodia. This morphology reflects the features of MAT. This suggesting that, CCG treatment inhibits mesenchymal migration, as cells appear to acquire the amoeboid migration mode.

In vivo studies using CCG-1423 from Ketchen (2019) identified that this inhibitor displays non-specific cytotoxicity within these studies. Therefore, modifications were made to the inhibitor to identify a less cytotoxic agent, being an analogue of CCG-1423 – CCG-203971. CCG-203971 was found to produce similar results as CCG-1423 in vitro, while also having an increased selectivity and potency. Therefore, it was subsequently taken further for in vivo GBM research. In the in vivo experiment, CCG- 203971 treatment of an implanted, patient-derived glioma cell line into a rodent model also showed promising results, being the first study to report the results of CCG-203971 in glioma research. The study suggests later research into increasing the drug dosage, or perhaps analysis of other CCG-1423 analogues for further study. These may have therapeutic potential as a combination treatment of GBM cell migration, as CCG-1423 has been shown to inhibit mesenchymal GBM cell migration, coupling the inhibitor with a drug targeting amoeboid migration may help inhibit migration completely.

Latrunculin A displays the greatest effect on decreasing cell migration in vitro

Of the four treatments used in this study, LAT A had the greatest effect in decreasing the migration distances from the GBM tumour spheroid. The morphological analysis indicated that there were large hypoxic regions in comparison to the other spheroid treatments, although there were only small regions of cell migration. The migrating cells appeared relatively spherical, and there were very few cells with an elongated cytoplasm.

As previously mentioned, LAT A acts as an actin-depolymerising agent within GBM cells, causing its anti-migratory effects through destabilisation of the cell cytoskeleton by targeting G-actin (Gandalovičová et al., 2017). Due to the mechanism of this drug, both mesenchymal and amoeboid migration modes are affected.

Literature surrounding the in vitro activity of LAT A in glioma cell lines, also supports the findings of this study. A study from Prahl et al. (2018), found that LAT A treatment decreased cell migration, decreasing further with an increased LAT A concentration. The study from Ketchen (2019), carried out a two-dimensional assay studying the migration distances of a range of inhibitors. The data indicated there was a significant decrease in cell migration when cells from the U251 cell line were treated with LAT A. As with the data obtained within this study, LAT A proved to be the most effective within the study over the other inhibitors used.

In vivo, assessment of the efficacy of LAT A in the treatment of GBM is yet to be established. However, there is currently literature surrounding the use of LAT A to treat gastric cancer in a rodent model. This study analysed the cytotoxic effect of LAT A, and showed it has a dose-dependent potency, decreasing cell viability with an increase in LAT A concentration. The survival rate in the model also increased as a result of this treatment (Konishi et al., 2009). Outside of cancer treatment, LAT A has been used to improve oocyte vitrification (through cytoskeletal stabilisation) within a clinical trial setting (U.S. National Library of Medicine, 2019). The results of this trial are yet

to be reported. Due to the promising results of LAT A in vitro for the treatment of GBM migration, further analysis of the therapeutic potential in vivo should be assessed.

Lithium chloride proves effective in vivo following combination treatment with Temozolomide

The final drug analysed within this study, LiCl, was shown to have the least effect of the inhibitors although still produced significant results in comparison to the control treatment. LiCl produced a similar mean migration distance to that of CCG-1423.

LiCl has been used clinically for the treatment of bipolar disorder for over 50 years. There are substantial amounts of literature surrounding the use of LiCl on glioma migration in comparison to the other treatments. Like BIO, LiCl is also an inhibitor of GSK-3β. A study from Nowicki et al. (2008) was the initial study focusing on the effect of Lithium (as part of LiCl) in vitro upon the U87 glioma cell line. The data indicated that lithium was able to decrease both the number of migrated cells, and the migrated distances travelled by these cells, supporting the outcome of this study. However, the data also suggests that LiCl treatment prevents the formation of cytoplasmic protrusions, indicating that the treatment may inhibit mesenchymal migration. This finding is different between the two studies, as the cell morphologies produced in response to the LiCl treatment appear different – the cells in this study appearing more elongated (Figure 13 and 14). Another study from Fu et al. (2014) also studies the in vitro effects of LiCl on the C6 glioma cell line. Migration was also inhibited through inhibition of GSK-3β.

In vivo, LiCl has been studied as a potential combination treatment with the chemotherapy drug, temozolomide (TMZ) in a study from Han et al. (2017). U87 cells were injected into the cranium of a nude mouse model. It was found that the doses of LiCl that inhibit migration were too high (outside the therapeutic window) within the serum and therefore led to toxicity. TMZ is also able to inhibit GSK-3β downstream. Therefore, for the treatment in vivo, TMZ was paired with low doses of LiCl. It was found that TMZ was able to potentiate the effects of the low concentration of LiCl. The study found that there was a prolonged survival within the mice models, as the tumour growth was reduced following the combination treatment. The survival outcome of the combination treatment was more effective than treatment of just TMZ or LiCl alone. Further development of this study may prove successful in improving the survival rates of patients diagnosed with GBM.

Alterations to this study for further research

To gain a more accurate understanding of how the treatments affect the cell migration mechanisms, alterations to the 'cell circularity index' study should be altered in QuPath. The alteration of cell morphology due to the change in migration modes in the migrating cells (seen in Figures 8 and 14), was not reflected in the 'cell circularity index' data (Figure 5). To more accurately study this in QuPath, mean average 'cell circularity index' for the migrated cells will be obtained from different sections around the tumour cell. Rings surrounding the tumour will allow for measurements to be obtained at different distances from the tumour. The 'cell circularity index' of the tumour spheroid should be obtained by using the same method as this study. Detection of the migrating cells should be adjusted so that there are four rings around the tumour. Figure 15 shows a suggested set-up for the 'cell circularity index' detections. Cell detections should occur within each of the four rings separately, at 25μm, 50μm, 100μm and 200μm away from the border of the tumour spheroid, obtaining only the data within each band produced and analysed within these distance brackets.

These rings will be drawn with the 'Ellipse' tool for the round spheroids. Spheroids which are not spherical, as seen in the BIO spheroids in Figure 9, will use the 'Polygon' tool to fit around the shape of the spheroid. Cells which do not fall within the 200µm ring will be detected and accounted for with the 'Wand' tool.

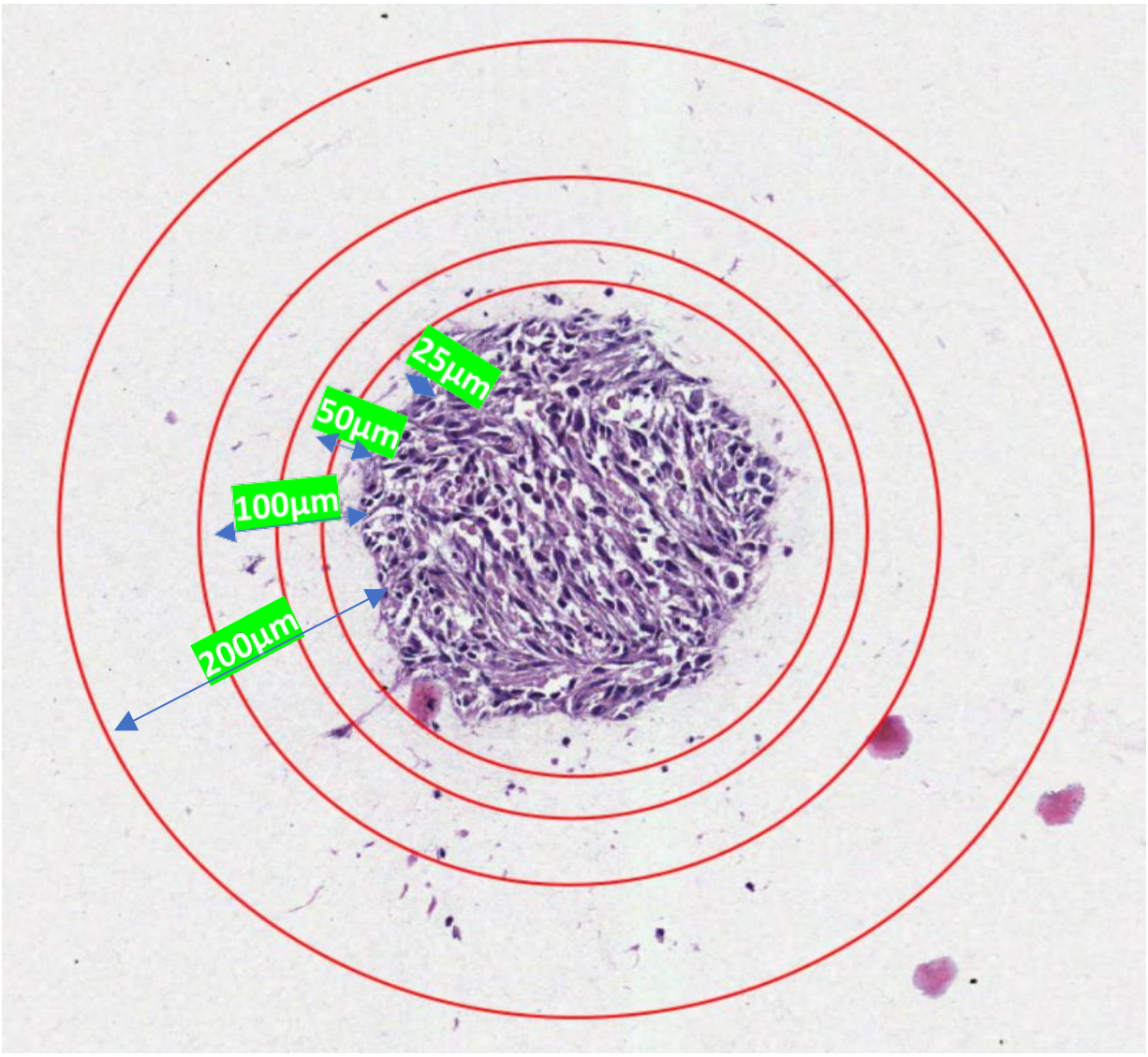

Figure 15: Control spheroid at x 10 magnification in QuPath. Rings at 25µm, 50µm, 100µm and 200µm away from the boarder of the spheroid will allow for a more accurate representation of the change in migration mode for the cell circularity index measurements

Conclusion

The results from this study clearly indicate the efficacy of the anti-migratory drugs used within this study, against GBM cell migration. The spheroid analysis focusing on the effect of these drugs upon the cell migration, showed significant results for each of the four drugs tested, as the mean average migration distance was decreased in each case, in comparison with the control. These results were clearly supported by the data obtained from the literature surrounding other in vitro studies of these drugs. Further studies of these drugs for in vivo assessment generally require alterations to improve their pharmacodynamic profile, to improve the potency and selectivity of these drugs to their relative inter-molecular target and decrease cytotoxicity. This particularly being the case for BIO and CCG-1423, producing BIA and CCG-20931 as their more effective derivatives in vivo, respectively. The potential for combination treatments of GBM using these drugs could prove effective, as seen with the use of TMZ with LiCl, and potentially increase the treatment options for patients suffering from GBM.

The determination of the 'cell circularity index' did not represent the results expected from the study. However, adaptations for further study were suggested to better understand the migrating cell morphology perhaps indicating the mode(s) of migration.

Acknowledgements

I would like to thank my supervisor, Dr Anke Brüning-Richardson, for her help and support throughout this project. Dr Brüning-Richardson's guidance and enthusiasm for the subject were instrumental to the development of this project, and I have thoroughly enjoyed working under her supervision.

I would also like to thank Dr Brüning-Richardson and her team for the laboratory preparation prior to this study, generating the data to be analysed within the project.

Glossary

Term	Definition	Page First Sited
Amoeboid (Migration)	A mode of glioma cell migration in which the cell appears more rounded in its morphology. Through this method, migrating cells squeeze between cells in the extracellular matrix in order to migrate. The faster mode of glioblastoma multiforme cell migration.	3
Astrocyte	A type of non-neuronal brain cell – supporting the function of neurones. Cancerous forms of asytrocytes form astrocytoma. High-grade astrocytomas form glioblastoma multiforme tumours.	2
Cytoskeleton	Provides cell structure – works to maintain the cell shape and transport substances inside cells.	3
Cytotoxic	Cell death or cellular damage as a result of a harmful process or substance.	2
Extracellular Matrix (ECM)	Fluid surrounding cells containing molecules, compounds and connective tissues forming a network among tissues.	3
Hypoxia/Hypoxic	Lack of oxygen.	3
In vitro	Isolated cell studies performed outside a biological organism (studied within laboratory equipment.)	1
In vivo	Cell studies performed within/implanted into a living biological organism (animal studies.)	1
Mesenchymal (Migration)	A mode of glioma cell migration in which cells appear elongated in its morphology. Cells using this mode of migration produce enzymes to degrade the surrounding extracellular matrix in order to migrate. This is the slower form of glioblastoma multiforme migration.	3
Necrosis	The death of cells within a tissue as a result of disease.	2
Parenchyma	The functional tissue of the brain.	3

References

Aiman, W., & Rayi, A. (2020). Low grade gliomas. In: StatPearls [Internet]. *Treasure island* (FL): StatPearls. https://www.ncbi.nlm.nih.gov/books/NBK560668/

Amin, N., & Vincan, E. (2012). The Wnt signaling pathways and cell adhesion. *Frontiers in Bioscience-Landmark*, *17*, 784–804. https://doi.org/10.2741/3957

Bankhead, P., Loughrey, M. B., Fernández, J. A., Dombrowski, Y., McArt, D. G., Dunne, P. D., McQuaid, S., Gray, R. T., Murray, L. J., Coleman, H. G., James, J. A., Salto-Tellez, M., & Hamilton, P. W. (2017). QuPath: Open source software for digital pathology image analysis. *Scientific Reports*, *7*(1), 16878. https://doi.org/10.1038/s41598-017-17204-5

Blažević, T., Heiss, E. H., Atanasov, A. G., Breuss, J. M., Dirsch, V. M., & Uhrin, P. (2015). Indirubin and indirubin derivatives for counteracting proliferative diseases. *Evidence-Based Complementary and Alternative Medicine*, 2015, 654098. https://doi.org/10.1155/2015/654098

Braig, S., Kressirer, C. A., Liebl, J., Bischoff, F., Zahler, S., Meijer, L., & Vollmar, A. M. (2013). Indirubin derivative 6BIO suppresses metastasis. *Cancer Research (Chicago, Ill.)*, *73*(19), 6004–12. https://10.1158/0008-5472.CAN-12-4358

Bronisz, A., Salińska, E., Chiocca, E. A., & Godlewski, J. (2020). Hypoxic roadmap of glioblastoma – learning about directions and distances in the brain tumor environment. *Cancers*, *12*(5), 1213. https://doi.org/10.3390/cancers12051213

Brown, D. V., Stylli, S. S., Kaye, A. H., & Mantamadiotis, T. (2019). Multilayered heterogeneity of glioblastoma stem cells: Biological and clinical significance. In A. Birbrair (Ed.), *Stem cells heterogeneity in cancer* (pp. 1–21). Springer International Publishing. https://doi.org/10.1007/978-3-030-14366-4_1

Brüning-Richardson, A., Droop, A., Tams, D., Boissinot, M., Hayes, J., Cheng, V., Cockle, J. V., Ismail, A., Morton, R., Esteves, F., Mittelbronn, M., Lawler, S., Short, S. C., & Mavria, G. (2018). Identification of transcriptional targets of GSK3 involved in glioblastoma invasion. *Neuro-Oncology*, *20*(S1), 26. https://doi.org/10.1093/neuonc/nox238.117

Cheng, V., Esteves, F., Chakrabarty, A., Cockle, J., Short, S., & Brüning-Richardson, A. (2015). High-content analysis of tumour cell invasion in three-dimensional spheroid assays. *Oncoscience*, *2*(6), 596–606. https://doi.org/10.18632/oncoscience.171

Claus, E. B., Walsh, K. M., Wiencke, J. K., Molinaro, A. M., Wiemels, J. L., Schildkraut, J. M., Bondy, M. L., Berger, M., Jenkins, R., & Wrensch, M. (2015). Survival and low-grade glioma: the emergence of genetic information. *Neurosurgical Focus*, *38*(1), E6. https://doi.org/10.3171/2014.10.FOCUS12367

Coué, M., Brenner, S. L., Spector, I., & Korn, E. D. (1987). Inhibition of actin polymerization by latrunculin A. *FEBS Letters*, *213*(2),316–18. https://doi.org/10.1016/0014-5793(87)81513-2

Croft, D. R., & Olson, M. F. (2011). Transcriptional regulation of Rho GTPase signaling. *Transcription*, *2*(5), 211–15. https://doi.org/10.4161/trns.2.5.16904

Dirven, L., Aaronson, N. K., Heimans, J. J., & Taphoorn, M. J. (2014). Health-related quality of life in high-grade glioma patients. *Chinese Journal of Cancer*, *33*(1), 40–5. https://doi.org/10.5732/cjc.013.10214

Evelyn, C. R., Bell, J. L., Ryu, J. G., Wade, S. M., Kocab, A., Harzdorf, N. L., Showalter, H. D., Neubig, R. R., & Larsen, S. D. (2010). Design, synthesis and prostate cancer cell- based studies of analogs of the Rho/MKL1 transcriptional pathway inhibitor, CCG-1423. *Bioorganic & Medicinal Chemistry Letters*, *20*(2), 665–72. https://doi.org/10.1016/j.bmcl.2009.11.056

Evelyn, C. R., Wade, S. M., Wang, Q., Wu, M., Iñiguez-Lluhí, J. A., Merajver, S. D., & Neubig, R. R. (2007). CCG-1423: a small-molecule inhibitor of RhoA transcriptional signaling. *Molecular Cancer Therapeutics*, *6*(8), 2249–60. https://doi.org/10.1158/1535-7163.MCT-06-0782

Fu, Y., Zheng, Y., Chan, K., Liang, A., & Hu, F. (2014). Lithium chloride decreases proliferation and migration of C6 glioma cells harboring isocitrate dehydrogenase 2 mutant via GSK-3β. *Molecular Biology Reports*, *41*(6), 3907–13. https://doi.org/10.1007/s11033-014-3258-7

Gandalovičová, A., Rosel, D., Fernandes, M., Veselý, P., Heneberg, P., Čermák, V., Petruželka, L., Kumar, S., Sanz-Moreno. V., & Brábek, J. (2017). Migrastatics – Anti-metastatic and anti-invasion drugs: Promises and challenges. *Trends in Cancer*, *3*(6), 391–406. https://10.1016/j.trecan.2017.04.008

Gau, D., Veon, W., Capasso, T. L., Bottcher, R., Shroff, S., Roman, B. L., & Roy, P. (2017). Pharmacological intervention of MKL/SRF signaling by CCG-1423 impedes endothelial cell migration and angiogenesis. *Angiogenesis*, *20*(4), 663–72. https://doi.org/10.1007/s10456-017-9560-y

Gupta, A., & Dwivedi, T. (2017). A simplified overview of World Health Organization classification update of central nervous system tumors 2016. *Journal of Neurosciences in Rural Practice*, *8*(4), 629–41. https://doi.org/10.4103/jnrp.jnrp_168_17

Han, S., Meng, L., Jiang, Y., Cheng, W., Tie, X., Xia, J., & Wu, A. (2017). Lithium enhances the antitumour effect of temozolomide against TP53 wild-type glioblastoma cells via NFAT1/FasL signalling. *British Journal of Cancer*, *116*(10), 1302–11. https://doi.org/10.1038/bjc.2017.89

Hanahan, D., & Weinberg, R. (2011). Hallmarks of cancer: The next generation. *Cell (Cambridge)*, *144*(5), 646–74. https://doi.org/10.1016/j.cell.2011.02.013

Ivkovic, S., Beadle, C., Noticewala, S., Massey, S. C., Swanson, K. R., Toro, L. N., Bresnick, A. R., Canoll, P., & Rosenfeld, S. S. (2012). Direct inhibition of myosin II effectively blocks glioma invasion in the presence of multiple motogens. *Molecular Biology of the Cell*, *23*(4), 533–42. https://doi.org/10.1091/mbc.E11-01-0039

Iwadate, Y. (2016). Epithelial-mesenchymal transition in glioblastoma progression. *Oncology Letters*, *11*(3), 1615–20. https://doi.org/10.3892/ol.2016.4113

Ketchen, S. E. (2019). Targeting the actin polymerisation pathway for improved treatment of glioblastoma [PhD Thesis, The University of Leeds]. https://etheses.whiterose.ac.uk/25184/

Kettenmann, H., Ransom, B. R., & Allen, N. J. (2013). *Neuroglia* (3rd ed.). New York: Oxford University Press.

Konishi, H., Kikuchi, S., Ochiai, T., Ikoma, H., Kubota, T., Ichikawa, D., Fujiwara, H., Okamoto, K., Sakakura, C., Sonoyama, T., Kokbuca, Y., Sasaki, H., Matsui, T., & Otsuji,

E. (2009). Latrunculin A has a strong anticancer effect in a peritoneal dissemination model of human gastric cancer in mice. *Anticancer Research*, *29*(6), 2091–7.

Li, H., Huang, K., Liu, X., Liu, J., Lu, X., Tao, K., Wang, G., & Wang, J. (2014). Lithium chloride suppresses colorectal cancer cell survival and proliferation through ROS/GSK-3β/NF-κB signaling pathway. *Oxidative Medicine and Cellular Longevity*, *2014*, 241864. https://doi.org/10.1155/2014/241864

Liu, C. A., Chang, C. Y., Hsueh, K. W., Su, H. L., Chiou, T. W., Lin, S. Z., & Harn, H. J. (2018). Migration/invasion of malignant gliomas and implications for therapeutic treatment. *International Journal of Molecular Sciences*, *19*(4), 1115. https://doi.org/10.3390/ijms19041115

Liu, L., Nam, S., Jove, R., Tian, Y., Yang, F., Wu, J., Wang, Y., Scuto, A., Polychronopolus, P., Magiatis, P., & Skaltsounis, L. (2011). 6-bromoindirubin-3'- oxime inhibits JAK/STAT3 signaling and induces apoptosis of human melanoma cells. *Cancer Research (Chicago, Ill.)*, *71*(11), 3972–9. https://doi.org/10.1186/1479-5876-8-112

Lu, Y., Sun, T., Chen, Y., Cai, Z., Zhao, J., Miao, F., Yang, Y., & Wang, S. (2020). Targeting the epithelial-to-mesenchymal transition in cancer stem cells for a better clinical outcome of glioma. *Technology in Cancer Research & Treatment*, *19*, https://doi.org/10.1177/1533033820948053

Manrique-Guzmán, S., Herrada-Pineda, T., & Revilla-Pacheco, F. (2017). Surgical management of glioblastoma. In: S. De Vleeschouwer (Ed.), *Glioblastoma*. https://doi.org/10.15586/codon.glioblastoma.2017.ch12

McCord, M., Mukouyama, Y., Gilbert, M. R., & Jackson, S. (2017). Targeting WNT signaling for multifaceted glioblastoma therapy. *Frontiers in Cellular Neuroscience*, *11*, 318. https://doi.org/10.3389/fncel.2017.00318

Meijer, L., Skaltsounis, A., Magiatis, P., Polychronopoulos, P., Knockaert, M., Leost, M., Ryan, X. P., Vonica, C. A., Brivanlou, A., Dajani, R., Crovace, C., Tarricone, C., Musacchio, A., Roe, S. M., Pearl, L., & Greengard, P. (2003). GSK-3-selective inhibitors derived from tyrian purple indirubins. *Chemistry & Biology*, *10*(12), 1255–66. https://doi.org/10.1016/j.chembiol.2003.11.010

Monteiro, A. R., Hill, R., Pilkington, G. J., & Madureira, P. A. (2017). The role of hypoxia in glioblastoma invasion. *Cells*, *6*(4), 45. https://doi.org/10.3390/cells6040045

Nager, M., Bhardwaj, D., Cantí, C., Medina, L., Nogués, P., & Herreros, J. (2012). B- catenin signalling in glioblastoma multiforme and glioma-initiating cells. *Chemotherapy Research and Practice*, *2012*, 192362–7. https://doi.org/10.1155/2012/192362

Nakada, M., Minamoto, T., Pyko, I. V., Hayashi, Y., & Hamada, J. (2011). The pivotal roles of GSK3β in glioma biology. InTech.

National Institute for Health and Clinical Excellence. (2005). Carmustine implants and temozolomide for the treatment of newly diagnosed high-grade glioma. nice.org.uk. https://www.nice.org.uk/guidance/ta121/documents/glioma-overview2

Naydenov, E., Tzekov, C., Minkin, K., Nachev, S., Romansky, K., & Bussarsky, V. (2011). Long-term survival with primary glioblastoma multiforme: a clinical study in Bulgarian patients. *Case Reports in Oncology*, *4*(1), 1–11. https://doi.org/10.1159/000323432

Nørøxe, D. S., Poulsen, H. S., & Lassen, U. (2017). Hallmarks of glioblastoma: a systematic review. *ESMO Open*, *1*(6), e000144. https://doi.org/10.1136/esmoopen-2016-000144

Nowicki, M. O., Dmitrieva, N., Stein, A. M., Cutter, J. L., Godlewski, J., Saeki, Y., Nita, M., Berens, M. E., Sander, L. M., Newton, H. B., Chiocca, E. A., & Lawler, S. (2008). Lithium inhibits invasion of glioma cells; possible involvement of glycogen synthase kinase-3. *Neuro-oncology*, *10*(5), 690–699. https://doi.org/10.1215/15228517-2008-041

Panková, K., Rösel, D., Novotný, M., & Brábek, J. (2010). The molecular mechanisms of transition between mesenchymal and amoeboid invasiveness in tumor cells. *Cellular and Molecular Life Sciences: CMLS*, *67*(1), 63–71. https://doi.org/10.1007/s00018-009-0132-1

Parri, M., & Chiarugi, P. (2010). Rac and Rho GTPases in cancer cell motility control. *ell Communication and Signaling : CCS*, *8*, 23. https://doi.org/10.1186/1478-811X-8-23

Phillips, H. S., Kharbanda, S., Chen, R., Forrest, W. F., Soriano, R. H., Wu, T. D., Misra, A., Nigro, J. M., Colman, H., Soroceanu, L., Williams, P. M., Modrusan, Z., Feuerstein, B. G., & Aldape, K. (2006). Molecular subclasses of high-grade glioma predict prognosis, delineate a pattern of disease progression, and resemble stages in neurogenesis. *Cancer Cell*, *9*(3), 157–73. https://doi.org/10.1016/j.ccr.2006.02.019

Prahl, L. S., Stanslaski, M. R., Vargas, P., Piel, M., & Odde, D. J. (2018). Glioma cell migration in confined microchannels via a motor-clutch mechanism. Cold Spring Harbor Laboratory. https://doi.org/10.1101/500843

Ransom, B. R., & Ransom, C. B. (2012) Astrocytes: multitalented stars of the central nervous system. In: R. Milner (Ed.), *Astrocytes. Methods in Molecular Biology (Methods and Protocols)*, vol 814. Humana Press. https://doi.org/10.1007/978-1-61779-452-0_1

Rohwedder, A., Knipp, S., Esteves, F. O., Hale, M., Treanor, D., & Brüning-Richardson, A. (2021) Three-dimensional (3D) reconstruction and cloudification of immunocytochemical sections of cancer spheroids for determination of quantitative parameters. (Manuscript in preparation.)

Roussos, E. T., Condeelis, J. S., & Patsialou, A. (2011). Chemotaxis in cancer. *Nature Reviews Cancer*, *11*(8), 573–87. https://doi.org/10.1038/nrc3078

Russell, J., Carlin, S., Burke, S. A., Wen, B., Yang, K. M., & Ling, C. C. (2009). Immunohistochemical detection of changes in tumor hypoxia. *International Journal of Radiation Oncology, Biology, Physics*, *73*(4), 1177–86. https://doi.org/10.1016/j.ijrobp.2008.12.004

Shevchenko, V., Arnotskaya, N., Korneyko, M., Zaytsev, S., Khotimchenko, Y., Sharma, H., & Bryukhovetskiy, I. (2019). Proteins of the Wnt signaling pathway as targets for the regulation of CD133+ cancer stem cells in glioblastoma. *Oncology Reports*, *41*, 3080–8. https://doi.org/10.3892/or.2019.7043

Sizoo, E. M., Braam, L., Postma, T. J., Pasman, H. R., Heimans, J. J., Klein, M., Reijneveld, J. C., & Taphoorn, M. J. (2010). Symptoms and problems in the end-of-life phase of high-grade glioma patients. *Neuro-Oncology*, *12*(11), 1162–6. https://doi.org/10.1093/neuonc/nop045

Song, Y., Zhang, Q., Kutlu, B., Difilippantonio, S., Bash, R., Gilbert, D., Yin, C., O'Sullivan, T. C., Yang, C., Kozlov, S., Bullitt, E., McCarthy, K. D., Kafri, T., Louis, D. N., Miller, C. R., Hood, L., & Van Dyke, T. (2013). Evolutionary etiology of high-grade astrocytomas. *Proceedings of the National Academy of Sciences - PNAS*, *110*(44), 17933–8. https://doi.org/10.1073/pnas.1317026110

Sun, T., Rodriguez, M., & Kim, L. (2009). Glycogen synthase kinase 3 in the world of cell migration. *Development, Growth & Differentiation*, *51*(9), 735–42. https://doi.org/10.1111/j.1440-169X.2009.01141.x

Symons, M., & Segall, J. E. (2009). Rac and Rho driving tumor invasion: who's at the wheel?. *Genome Biology*, *10*(3), 213. https://doi.org/10.1186/gb-2009-10-3-213

Talkenberger, K., Cavalcanti-Adam, E. A., Voss-Böhme, A., & Deutsch, A. (2017). Amoeboid-mesenchymal migration plasticity promotes invasion only in complex heterogeneous microenvironments. *Scientific Reports*, *7*(1), 9237. https://doi.org/10.1038/s41598-017-09300-3

Urbańska, K., Sokołowska, J., Szmidt, M., & Sysa, P. (2014). Glioblastoma multiforme - an overview. *Contemporary Oncology (Poznan, Poland)*, *18*(5), 307–12. https://doi.org/10.5114/wo.2014.40559

U.S. National Library of Medicine. (2019). Oocyte Vitrification Aided With Latrunculin A. clinicaltrials.gov. https://clinicaltrials.gov/ct2/show/study/NCT03678571

Villanueva-Meyer, J. E., Mabray, M. C., & Cha, S. (2017). Current clinical brain tumor imaging. *Neurosurgery*, *81*(3), 397–415. https://doi.org/10.1093/neuros/nyx103

Walid, M. S. (2008). Prognostic factors for long-term survival after glioblastoma. *The Permanente Journal*, *12*(4), 45–8. https://doi.org/10.7812/tpp/08-027

Williams, S. P., Nowicki, M. O., Liu, F., Press, R., Godlewski, J., Abdel-Rasoul, M., Kaur, B., Fernandez, S. A., Chiocca, E. A., & Lawler, S. E. (2011). Indirubins decrease glioma invasion by blocking migratory phenotypes in both the tumor and stromal endothelial cell compartments. *Cancer Research (Chicago, Ill.)*, *71*(16), 5374–80. https://doi.org/10.1158/0008-5472.CAN-10-3026

Wippold, F. J., II, Lammle, M., Anatelli, F., Lennerz, J., & Perry, A. (2006). Neuropathology for the neuroradiologist: Palisades and pseudopalisades. *American Journal of Neuroradiology : AJNR*, *27*(10), 2037–41.

Yarmola, E. G., Somasundaram, T., Boring, T. A., Spector, I., & Bubb, M. R. (2000). Actin-latrunculin A structure and function. differential modulation of actin-binding protein function by latrunculin A. *The Journal of Biological Chemistry*, *275*(36), 28120–7. https://doi.org/10.1074/jbc.M004253200

Zepecki, J. P., Snyder, K. M., Moreno, M. M., Fajardo, E., Fiser, A., Ness, J., Sarkar, A., Toms, S. A., & Tapinos, N. (2019). Regulation of human glioma cell migration, tumor growth, and stemness gene expression using a lck targeted inhibitor. *Oncogene*, *38*(10), 1734–50. https://doi.org/10.1038/s41388-018-0546-z

Zhan, J. S., Gao, K., Chai, R. C., Jia, X. H., Luo, D. P., Ge, G., Jiang, Y. W., Fung, Y. W., Li, L., & Yu, A. C. (2017). Astrocytes in Migration. *Neurochemical Research*, *42*(1), 272– 82. https://doi.org/10.1007/s11064-016-2089-4

Zhang, X., Castanotto, D., Nam, S., Horne, D., & Stein, C. (2017). 6BIO enhances oligonucleotide activity in cells: A potential combinatorial anti-androgen receptor therapy in prostate cancer cells. *Molecular Therapy*, *25*(1), 79–91. https://doi.org/10.1016/j.ymthe.2016.10.017

Zhong, J., Paul, A., Kellie, S. J., & O'Neill, G. M. (2010). Mesenchymal migration as a therapeutic target in glioblastoma. *Journal of Oncology*, https://doi.org/10.1155/2010/430142

Appendices

Appendix 1: Descriptive statistics for the migration measurements obtained from SPSS. Mean and standard error of the mean values are highlighted. CONTROL_MMeasurements = Control spheroid migration measurements, CCG_MMeasurements = CCG inhibiotor spheroid migration measurements, BIO_MMeasurements = Bio-indirubin spheroid migration measurements, LiCl_MMeasurements = Lithium Chloride spheroid migration measurements, LATA_MMeasurements = Latrunculin A spheroid migration measurements

Statistics

CONTROL_MMeasurements			CCG_MMeasurements	BIO_MMeasurements	LiCl_MMeasurements	LATA_MMeasurements
N	Valid	3104	628	736	2476	409
	Missing	0	2476	2368	628	2695
Mean		102.7330	40.5409	32.0407	41.0664	16.9537
Std. Error of Mean		1.69950	1.73492	1.14457	.71835	.65283
Median		77.3800	22.0900	24.2650	31.5500	13.7500
Mode		13.19[a]	14.13	16.45	6.37[a]	7.81[a]
Std. Deviation		94.68491	43.47702	31.05132	35.74458	13.20265
Variance		8965.233	1890.251	964.185	1277.675	174.310
Range		785.50	174.65	239.46	226.50	74.87
Minimum		.19	.82	.63	.53	.40
Maximum		785.69	175.47	240.09	227.03	75.27
Sum		318883.19	25459.67	23581.94	101680.35	6934.06

a. Multiple modes exist. The smallest value is shown

Appendix 2: Kruskal-Wallis comparing the differences between the spheroid treatments - control, Bio-indirubin, CCG inhibitor, Lithium chloride and Latrunculin A

Test Statistics[a,b]

Measurements

1.

Kruskal-Wallis H	1578.675
df	4
Asymp. Sig.	.000

a. Kruskal Wallis Test

b. Grouping Variable: Treatment

Appendix 3: Post-hoc analysis – pairwise comparisons of different spheroid treatment migratin distances. Significant values are highlighted. BIO = Bio-indirubin, CCG = CCG inhibitor, CON = Control, LATA = Latrunculin A, LiCl = Lithium Chloride.

Pairwise Comparisons of Treatment

Sample 1-Sample 2	Test Statistic	Std. Error	Std. Test Statistic	Sig.	Adj. Sig.[a]
LAT A-BIO	901.675	130.920	6.887	.000	.000
LAT A-CCG	1076.458	134.881	7.981	.000	.000
LAT A-LiCl	-1402.450	113.302	-12.378	.000	.000
LAT A-Control	3016.678	111.666	27.015	.000	.000
BIO-CCG	-174.783	115.317	-1.516	.130	1.000
BIO-LiCl	-500.775	89.120	-5.619	.000	.000
BIO-Control	2115.003	87.030	24.302	.000	.000
CCG-LiCl	-325.992	94.844	-3.437	.001	.006
CCG-Control	1940.220	92.882	20.889	.000	.000
LiCl-Control	1614.228	57.198	28.222	.000	.000

Each row tests the null hypothesis that the Sample 1 and Sample 2 distributions are the same.

Asymptotic significances (2-sided tests) are displayed. The significance level is .05.

a. Significance values have been adjusted by the Bonferroni correction for multiple tests.

Appendix 4: Descriptive statistics for the cell circularity data. Mean values and standard error of the mean are highlighted. Mig = migrated cell circularity, Tum = tumour cell circularity, BIO = Bio-indirubin, CCG = CCG inhibitor, CON = Control, LATA = Latrunculin A, LiCl = Lithium Chloride.

Descriptive Statistics

	N	Minimum	Maximum	Mean		Std. Deviation
	Statistic	Statistic	Statistic	Statistic	Std. Error	Statistic
BIO_Mig_Cells	2280	.5000	.9887	.867350	.0017720	.0846135
BIO_Tum_Cells	50608	.4448	.9829	.796926	.0003372	.0758512
CCG_Mig_Cells	1147	.5212	.9890	.880442	.0023404	.0792649
CCG_Tum_Cells	41364	.3802	.9815	.790059	.0003875	.0788057
CON_Mig_Cells	4737	.4497	.9916	.867450	.0012318	.0847792
CON_Tum_Cells	40575	.3796	.9716	.782842	.0004072	.0820201
LATA_Mig_Cells	1107	.5525	.9914	.877140	.0024213	.0805603
LATA_Tum_Cells	20390	.4766	.9791	.804629	.0005070	.0723941
LiCl_Mig_Cells	4035	.5500	.9901	.870905	.0012351	.0784538